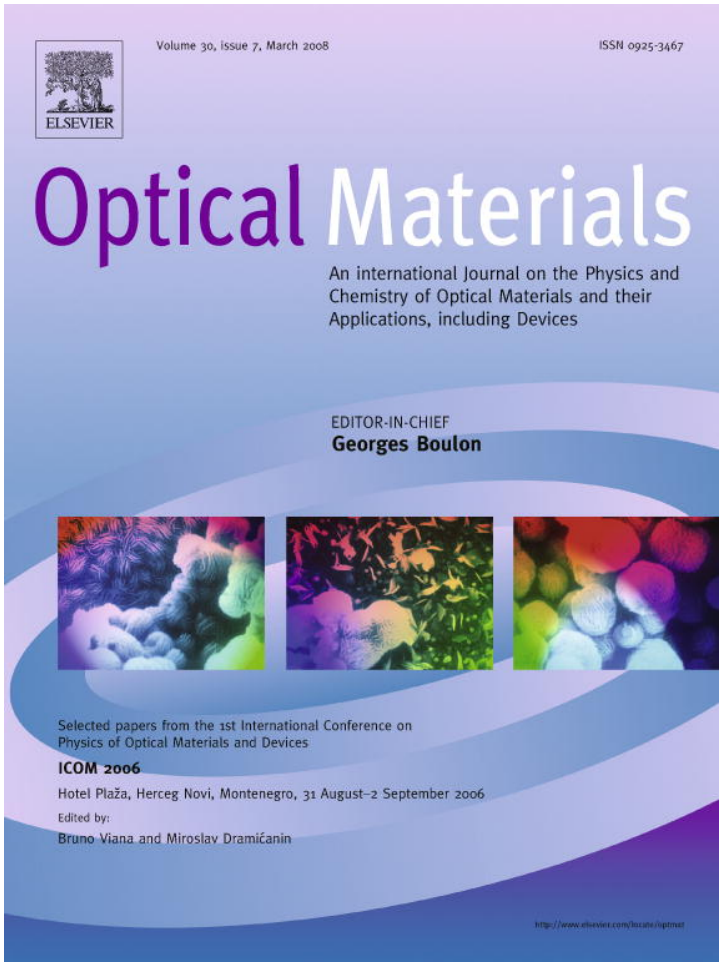

Available online at www.sciencedirect.com
ScienceDirect
Optical Materials 30 (2008) 1173–1176
OPTICAL Materials
www.elsevier.com/locate/optmat

Counterpropagating beams in rotationally symmetric photonic lattices

Dragana Jović [a,*], Raka Jovanović [a], Slobodan Prvanović [a], Milan Petrović [a], Milivoj Belić [b]

[a] Institute of Physics, P.O. Box 57, 11001 Belgrade, Serbia
[b] Texas A&M University at Qatar, P.O. Box 5825, Doha, Qatar

Available online 12 July 2007

Abstract

Various properties of counterpropagating mutually incoherent self-trapped beams in optically induced circular photonic lattices with ring defects are investigated numerically. We utilize a local isotropic dynamical model with a Kerr-type saturable nonlinearity. Different incident beam structures are considered. We find spontaneous symmetry breaking of the head-on propagating Gaussian beams. In the case of vortices, we observe beam filamentation and a strong pinning of filaments to the lattice sites. Using a modified Petviashvili's method, we report several novel solitonic structures.

PACS: 42.65.Tg; 42.65.Sf

Keywords: Circular photonic lattices; Ring defects; Solitonic structures

1. Introduction

Optically induced photonic lattices attracted a lot of interest recently, owing to intriguing waveguiding possibilities [1]. Until recently, only simple stationary structures have been described theoretically and generated experimentally in optically induced lattices [2]. Optical lattices tend to suppress rich instability-induced dynamics (rotating, diverging, and self-bending) of beam filaments in a homogeneous nonlinear medium. Up to now different two-dimensional lattices have been considered [1–4]. In this paper we choose circular photonic lattices (CPL) with ring defects, with an intention of locating and investigating novel dynamical, as well as stable optical structures. We investigate numerically the properties of counterpropagating (CP) mutually incoherent self-trapped beams in optically induced fixed CPL, and determine the conditions for observing solitonic solutions.

2. Modelisation

The behavior of CP beams in photonic lattices is described by a time-dependent model for the formation of self-trapped CP optical beams, based on the theory of photorefractive (PR) effect. The model consists of wave equations in the paraxial approximation for the propagation of CP beams and a relaxation equation for the generation of the space charge field in the PR crystal, in the isotropic approximation. The model equations in the computational space are of the form:

$$\mathrm{i}\partial_z F = -\Delta F + \Gamma E F, \quad -\mathrm{i}\partial_z B = -\Delta B + \Gamma E B, \tag{1}$$

$$\tau\partial_t E + E = -\frac{I + I_g}{1 + I + I_g}, \tag{2}$$

where F and B are the forward and the backward propagating beam envelopes, Δ is the transverse Laplacian, Γ is the dimensionless coupling constant, τ is the relaxation time of the crystal, and E the homogenous part of the space charge field. The quantity $I = |F|^2 + |B|^2$ is the laser light intensity, measured in units of the background intensity. I_g is the transverse intensity distribution of the optically induced lattice array. It is formed by positioning Gaussian beams

* Corresponding author. Tel.: +381 11 3160260; fax: +381 11 3162190.
E-mail address: jovic@phy.bg.ac.yu (D. Jović).

0925-3467/$ - see front matter © 2007 Elsevier B.V. All rights reserved.
doi:10.1016/j.optmat.2007.05.054

at the sites of the lattice, and is normalized by the dark irradiance I_d. A scaling $x/x_0 \to x$, $y/x_0 \to y$, $z/L_D \to z$, is utilized in the writing of dimensionless propagation equations, where x_0 is the typical FWHM beam waist and L_D is the diffraction length. The propagation equations are solved numerically, concurrently with the temporal equation, in the manner described in Ref. [5] and references cited therein.

For the lattice array we choose a circular arrangement of beams [3], with ring defects. The distance between lattice sites is constant in each concentric circle, but slightly differs in different circles. The ratio between the distance of neighboring lattice sites in the first circle and the FWHM of lattice beams is chosen to be 2.05. The beams are assumed to be degenerate and incoherent in the forward and backward components.

3. Counterpropagating Gaussian and vortex beams

We investigate the interaction of CP Gaussian and vortex beams in a seven-fold symmetric CPL with two ring defects. For the Gaussian–Gaussian interaction we choose CPL with the first and the third ring missing, and with FWHM of the input beams corresponding to the radii of the missing rings. First, we consider CP Gaussians with the same width (Fig. 1). When FWHM of the input beams corresponds to the radius of the first missing ring, the observed structures are stable and pinned to the central lattice beam (left column). For the input beam's FWHM that corresponds to the radius of the second defect, we get regular dynamics at the beginning, but unstable behavior afterwards (right column).

Next, we consider CP Gaussians with different widths (Fig. 2). We choose the forward beam to be narrower (whose FWHM corresponds to the radius of the first missing ring) than the backward beam (whose FWHM corresponds to the radius of the second missing ring). A general result is the appearance of different stable filamented structures with several parts, in the form of stand-

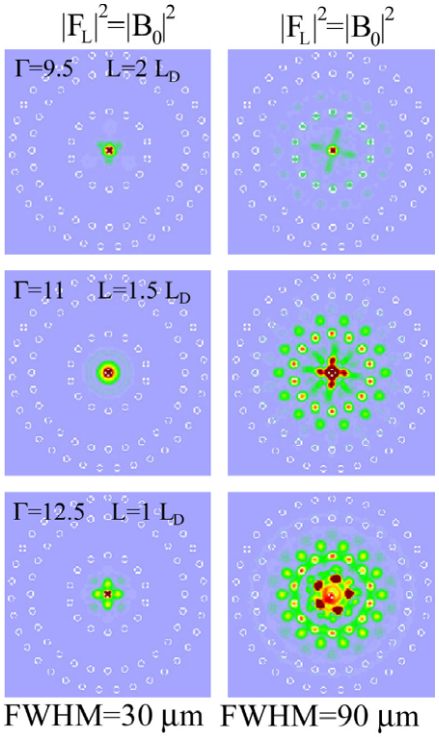

Fig. 1. Gaussian–Gaussian interaction of CP components with the same width: intensity distributions of the forward (backward) field at its output face, for FWHM = 30 μm (left column) and FWHM = 90 μm (right column), and for various values of the control parameter ΓL. Parameters: lattice spacing 30 μm, FWHM of lattice beams 9 μm, maximum lattice intensity $I_g = 5I_d$, $|F_0|^2 = |B_L|^2 = 1$.

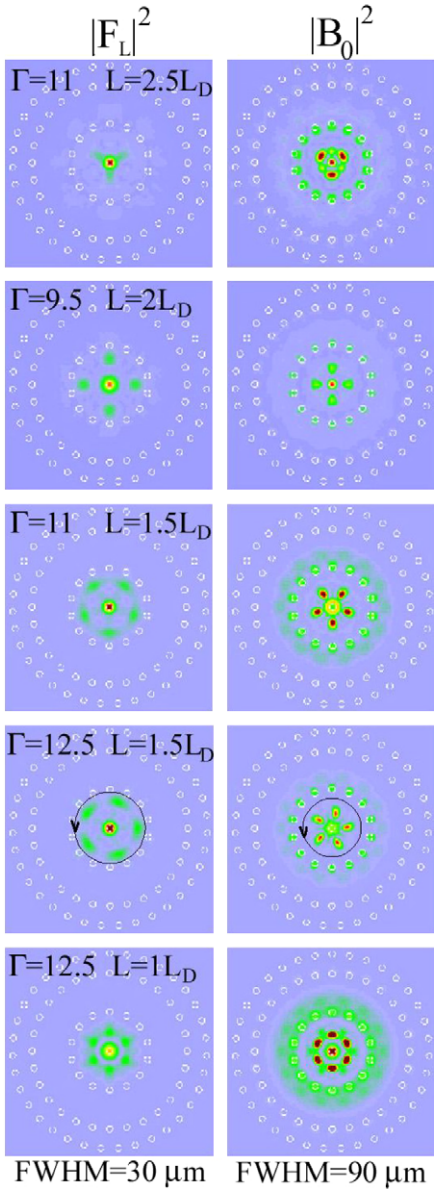

Fig. 2. Gaussian–Gaussian interaction of CP components with different widths: intensity distributions of the forward beam with FWHM = 30 μm (left column) and of the backward beam with FWHM = 90 μm (right column), for various values of the control parameter ΓL. Other parameters are as in Fig. 1.

ing waveguides. For particular values of control parameters Γ and L, we observe stable dynamical structures, such as the rotating five-fold structure (the fourth row). In all the cases considered, the narrower beam is strongly pinned to the central lattice site, whereas the wider one is more spread out.

For the vortex–vortex interaction we choose CPL with the second and the fourth ring missing, and also with the central lattice beam absent. We consider the case with two identical CP vortices, and vary only their input FWHM (Fig. 3). For the beams with FWHM equal to 30, 45 and 60 μm, we observe almost regular rotation of vortex filaments. In the case of FWHM = 75 μm, we find stable structure strongly pinned to the lattice sites. For wider vortices (90 and 120 μm) unstable structures appear.

Finally, we investigate different combinations of interacting Gaussians and vortices, with various widths (Fig. 4). We choose CPL with the second and the fourth ring missing, and FWHM of the input beams corresponding to the radii of the ring defects. In the case of interacting Gaussians (first row), the wider beam can regenerate the missing second lattice ring, which is not the case for another situations. For the Gaussian–vortex interactions, the narrower vortex filaments only to the nearest lattice sites in the first ring (second row), while the broader vortex acquires a more complex structure (third row). Both interacting vortices (fourth row) do not preserve their form, filamenting into a seven-fold structure. It is interesting to note that Gaussians possess phase distributions which correspond to the group symmetry of the lattice (C7), even in the case of Gaussian–Gaussian interaction. Vortices display the typical phase distribution, characteristic of vortices with the opposite topological charges $(1, -1)$ (fourth row).

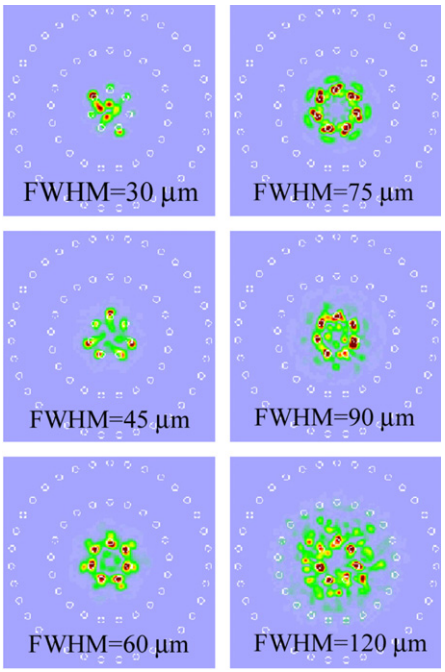

Fig. 3. Intensity distributions of the backward vortex field at its output face, for various FWHM of the input beams and for $\Gamma = 17$, $L = 1.5L_D = 6$ mm. Other parameters are as in Fig. 1.

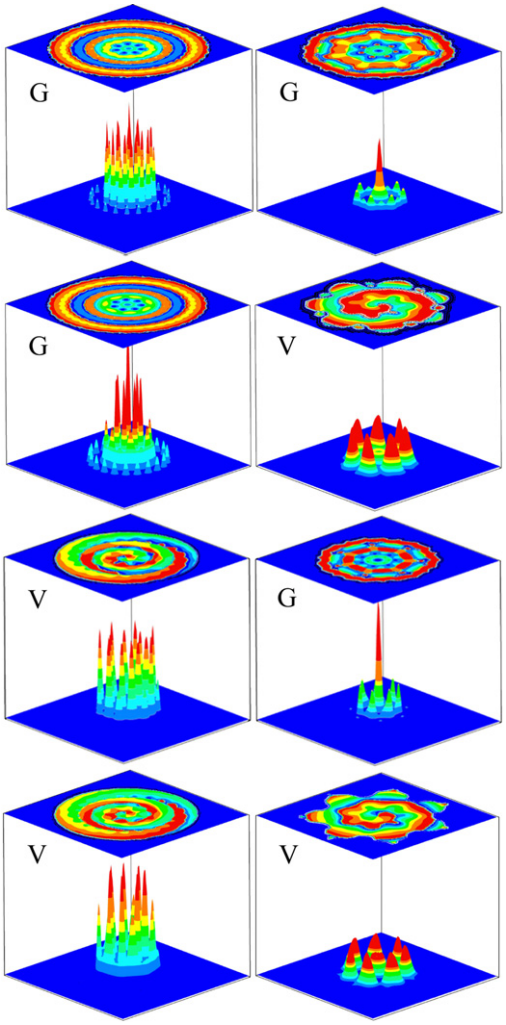

Fig. 4. Intensity (bottom) and phase (top) distributions of different combinations of the interacting Gaussians (G) and vortices (V), arranged in 4 rows, for two values of FWHM (the first column 120 μm, the second column 60 μm). Parameters: $\Gamma = 11$, $L = 1L_D$; other parameters are as in Fig. 1.

4. Solitonic solutions

To investigate solitonic solutions in CPL, we consider Eqs. (1) and (2) in the steady-state. Because of the rotational symmetry, the above equations suggest the existence of fundamental vector solitons, in the form [4]:

$$F = u(x, y)\cos\theta\exp(\mathrm{i}\mu z), \tag{3}$$

$$B = u(x, y)\sin\theta\exp(-\mathrm{i}\mu z), \tag{4}$$

where θ is an arbitrary projection angle, and μ is the propagation constant. Eq. (1) in the steady-state are transformed into the same (degenerate) equation:

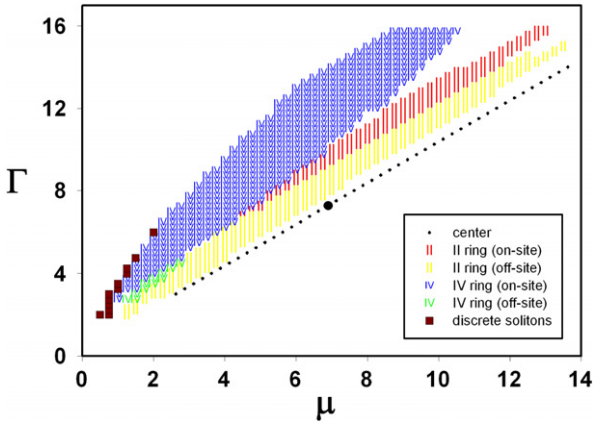

Fig. 5. Different kinds of solitonic solutions in the Γ–μ plane. Lattice parameters are as in Fig. 1. The inset lists possible soliton positions in the lattice where the solitons are localized.

$$\mu u + \Delta u + \Gamma u \frac{|u|^2 + I_g}{1 + |u|^2 + I_g} = 0. \quad (5)$$

Solitonic solutions can be found from Eq. (5) using the modified Petviashvili's method. Of course, the CP beams can not form a soliton if the medium is too long [6].

We investigate the form of the solitonic solutions in a seven-fold symmetric CPL with the first and the third ring missing. We find three basic kinds of solitons: the on-site solitons (localized at the lattice sites), the off-site solitons (localized between the lattice sites) and the discrete solitons (spread over many sites). The on-site solitons are localized on the second or fourth rings, the off-site solitons are localized in-between the second (fourth) lattice ring sites, and the less localized, discrete solitonic structures are spread over many sites in the fourth and fifth rings. The distribution of different solitonic solutions over the regions in the Γ–μ plane is presented in Fig. 5. In addition to these typical solitonic structures, there exist quasi-stable localized structures at the position of the lattice's central beam (dot–dot line in the Γ–μ plane). The most stable soliton structure there appears for $\Gamma = 7.27$ and $\mu = 6.9$. Typical intensity distributions of all the solitonic solutions are presented in Fig. 6.

5. Conclusion

We investigated numerically properties of the counter-propagating mutually incoherent self-trapped beams in optically induced circular photonic lattices with ring defects. We observed spontaneous symmetry breaking of the head-on propagating Gaussian beams, and regular rotation of CP Gaussian filaments. In the case of vortices, we found beam filamentation, a strong pinning of filaments to the lattice sites, and irregular behavior. Using the modified Petviashvili's method, we determined the conditions in the parameter plane for observing solitons, and identified different families of such solitonic solutions. Similar effects can be expected in photonic crystal fibers.

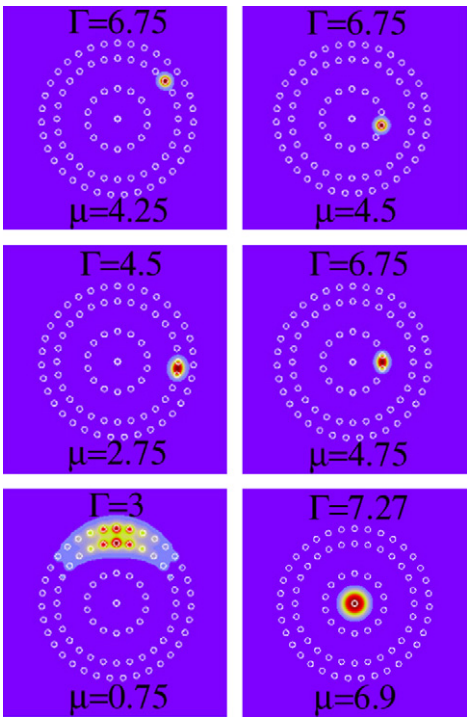

Fig. 6. Intensity distributions for all typical solitonic solutions: The on-site solitons (first row), the off-site solitons (second row), the discrete solitons (third row, left), and the lattice central beam soliton (third row, right).

Acknowledgements

Work at the Institute of Physics is supported by the Ministry of Science and Environmental Protection of the Republic of Serbia, under the Project OI 141031. We are thankful to the IT Center of the Texas A&M University at Qatar, for allowing us to use the SAQR supercomputing cluster.

References

[1] Y.S. Kivshar, G.P. Agrawal, Optical Solitons, Academic Press, San Diego, 2003.
[2] J. Fleischer, M. Segev, N. Efremidis, D. Christodoulides, Nature 422 (2003) 147.
[3] S. Xiao, M. Qiu, Photon. Nanostruct. – Fundam. Appl. 3 (2005) 134.
[4] Z. Chen, A. Bezryadina, I. Makasyuk, J. Yang, Opt. Lett. 29 (2004) 1656.
[5] M. Belić, M. Petrović, D. Jović, A. Strinić, D. Arsenović, K. Motzek, F. Kaiser, Ph. Jander, C. Denz, M. Tlidi, P. Mandel, Opt. Express 12 (2004) 708.
[6] K. Motzek, Ph. Jander, A. Desyatnikov, M. Belić, C. Denz, F. Kaiser, Phys. Rev. E 68 (2003) 066611.